Synthesis and Properties of T-Cage-Type S-Bridged Rh^{III}Zn^{II} Octanuclear Complexes with 2-Aminoethanethiolate or L-Cysteinate

Takumi Konno,* Ken-ichi Okamoto, and Jinsai Hidaka

Department of Chemistry, University of Tsukuba, Tsukuba, Ibaraki 305, Japan

Received June 4, 1993[⊛]

The reactions of $fac(S)$-[Rh(aet)$_3$] or Δ_{LLL}-$fac(S)$-[Rh(L-cys-N,S)$_3$]$^{3-}$ with a mixture of Zn^{2+} and ZnO in water produced T-cage-type S-bridged octanuclear complexes with a [Zn$^{II}_4$O]$^{6+}$ core, [{Rh(aet)$_3$}$_4$Zn$_4$O]$^{6+}$ (**1**) and $\Delta_{LLL}\Delta_{LLL}\Delta_{LLL}\Delta_{LLL}$-[{Rh(L-cys-$N,S$)$_3$}$_4Zn_4$O]$^{6-}$ (**2**). A similar T-cage-type complex with a [Zn$^{II}_{3.7}$Co$^{II}_{0.3}$O]$^{6+}$ core, [{Rh(aet)$_3$}$_4$Zn$_{3.7}$Co$_{0.3}$O]$^{6+}$ (**3**), was derived from a linear-type S-bridged trinuclear complex, [Co^{III}{Rh(aet)$_3$}$_2$]$^{3+}$, by reacting with Zn powder in water, followed by adding Zn^{2+}. The chloride, bromide, and nitrate salts of **1** and **3** were commonly subject to spontaneous resolution to give only two isomers, (+)$^{CD}_{350}$-$\Lambda\Lambda\Lambda\Lambda$ and (−)$^{CD}_{350}$-$\Delta\Delta\Delta\Delta$. The crystal structure and absolute configuration of the (−)$^{CD}_{350}$ isomer for each of **1**Br$_6$ and **3**Br$_6$ were determined by X-ray crystallography. (−)$^{CD}_{350}$-**1**Br$_6$·9H$_2$O crystallizes in the cubic space group $P2_13$ with a = 19.017(1) Å, V = 6876.9(4) Å^3, Z = 4, R = 0.0519, and R_w = 0.0475. (−)$^{CD}_{350}$-**3**Br$_6$·8H$_2$O also crystallizes in the cubic space group $P2_13$ with a = 18.922(1) Å, V = 6775.3(4) Å^3, Z = 4, R = 0.0495, and R_w = 0.0430. In **1** the four octahedral $fac(S)$-[Rh(aet)$_3$] subunits are bound to the tetrahedral [Zn$_4$O]$^{6+}$ core in a tetrahedral arrangement, and each Zn(II) is tetrahedrally coordinated by three thiolato sulfur atoms from three different $fac(S)$-[Rh(aet)$_3$] subunits and a central μ_4-oxygen atom. The chiral configurations are regulated to Δ for all four $fac(S)$-[Rh(aet)$_3$] subunits and R for all 12 asymmetric bridging sulfur atoms in the (−)$^{CD}_{350}$ isomer of **1**, giving a T symmetrical structure. While (−)$^{CD}_{350}$-**3** was isostructural with (−)$^{CD}_{350}$-**1**, the plasma emission analysis and electronic absorption spectrum indicated that a slight amount of Co(II) is trapped in place of Zn(II) in **3** (Zn:Co = 3.7:0.3). The absorption and circular dichroism (CD) spectral behavior of the present T-cage-type Rh^{III}Zn^{II} octanuclear complexes are discussed in comparison with those of the mononuclear $fac(S)$-[Rh(aet)$_3$] and Δ_{LLL}-$fac(S)$-[Rh(L-cys-N,S)$_3$]$^{3-}$ complexes.

Introduction

Over the past three decades there has been considerable attention toward the study of S-bridged polynuclear complexes with 2-aminoethanethiolate (aet = NH$_2$CH$_2$CH$_2$S$^-$) or L-cysteinate (L-cys = NH$_2$CH(COO$^-$)CH$_2$S$^-$).[1–9] In particular, S-bridged polynuclear complexes composed of chiral $fac(S)$-[M(aet)$_3$]$^{2,4-9}$ or $fac(S)$-[M(L-cys-N,S)$_3$]$^{3-}$ ^{3,4} (M = Co(III), Rh-

* Abstract published in *Advance ACS Abstracts*, January 1, 1994.

(1) (a) Jicha, D. C.; Busch, D. H. *Inorg. Chem.* **1962**, *1*, 872. (b) Jicha, D. C.; Busch, D. H. *Inorg. Chem.* **1962**, *1*, 878. (c) Wei, C. H.; Dahl, L. F. *Inorg. Chem.* **1970**, *9*, 1878. (d) Artz, R. J.; Blinn, E. L.; Newman, D. S. *Inorg. Nucl. Chem.* **1973**, *35*, 2831. (e) Lane, R. H.; Pantaleo, N. S.; Farr, J. K.; Coney, W. M.; Newton, M. G. *J. Am. Chem. Soc.* **1978**, *100*, 1610. (f) Kang, D.; Poor, M.; Blinn, E. L. *Inorg. Chim. Acta* **1990**, *168*, 209. (g) Konno, T.; Okamoto, K.; Hidaka, J. *Inorg. Chem.* **1992**, *31*, 160.

(2) (a) Busch, D. H.; Jicha, D. C. *Inorg. Chem.* **1962**, *1*, 884. (b) Brubaker, G. R.; Douglas, B. E. *Inorg. Chem.* **1967**, *6*, 1562. (c) DeSimone, R. E.; Ontko, T.; Wardman, L.; Blinn, E. L. *Inorg. Chem.* **1975**, *14*, 1313. (d) Blinn, E. L.; Butler, P.; Chapman, K. M.; Harris, S. *Inorg. Chim. Acta* **1977**, *24*, 139. (e) Brubaker, G. R.; Henk, M. G.; Johnson, D. W. *Inorg. Chim. Acta* **1985**, *100*, 201. (f) Heeg, M. J.; Blinn, E. L.; Deutsch, E. *Inorg. Chem.* **1985**, *24*, 1118. (g) Johnson, D. W.; Brewer, T. R. *Inorg. Chim. Acta* **1988**, *154*, 221. (h) Miyanowaki, S.; Konno, T.; Okamoto, K.; Hidaka, J. *Bull. Chem. Soc. Jpn.* **1988**, *61*, 2987. (i) Konno, T.; Okamoto, K.; Hidaka, J. *Acta Crystallogr.* **1993**, *C49*, 222.

(3) (a) Konno, T.; Aizawa, S.; Okamoto, K.; Hidaka, J. *Chem. Lett.* **1985**, 1017. (b) Okamoto, K.; Aizawa, S.; Konno, T.; Einaga, H.; Hidaka, J. *Bull. Chem. Soc. Jpn.* **1986**, *59*, 3859. (c) Aizawa, S.; Okamoto, K.; Einaga, H.; Hidaka, J. *Bull. Chem. Soc. Jpn.* **1988**, *61*, 1601.

(4) (a) Konno, T.; Aizawa, S.; Hidaka, J. *Bull. Chem. Soc. Jpn.* **1989**, *62*, 585. (b) Konno, T.; Aizawa, S.; Okamoto, K.; Hidaka, J. *Bull. Chem. Soc. Jpn.* **1990**, *63*, 792. (c) Konno, T.; Okamoto, K.; Hidaka, J. *Bull. Chem. Soc. Jpn.* **1990**, *63*, 3027. (d) Konno, T.; Nakamura, K.; Okamoto, K.; Hidaka, J. *Bull. Chem. Soc. Jpn.* **1993**, *66*, 2582.

(5) (a) Konno, T.; Okamoto, K.; Hidaka, J. *Chem. Lett.* **1990**, 1043. (b) Konno, T.; Okamoto, K.; Hidaka, J. *Bull. Chem. Soc. Jpn.*, in press.

(6) Konno, T.; Okamoto, K.; Hidaka, J. *Inorg. Chem.* **1991**, *30*, 2253.

(7) Konno, T.; Nagashio, T.; Okamoto, K.; Hidaka, J. *Inorg. Chem.* **1992**, *31*, 1160.

(8) Okamoto, K.; Konno, T.; Kageyama, Y.; Hidaka, J. *Chem. Lett.* **1992**, 1105.

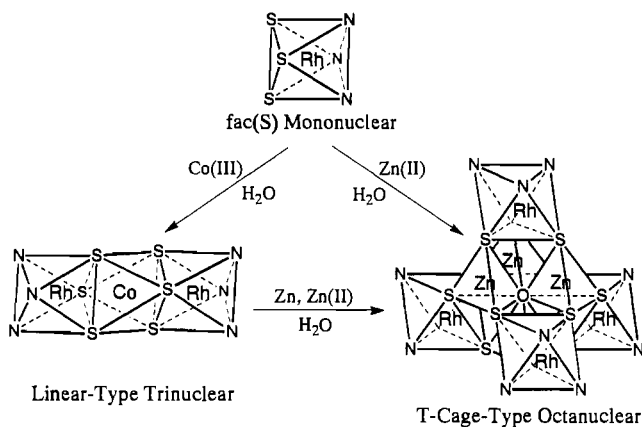(9) Konno, T.; Okamoto, K.; Hidaka, J. *Inorg. Chem.* **1992**, *31*, 3875.

(III), Ir(III)) subunits are of special interest, because of their diverse and specific stereochemical behavior. It has been recognized that the mononuclear $fac(S)$-[M(aet or L-cys-N,S)$_3$]$^{0,3-}$ complexes can function as a S-donating tridentate ligand, and a number of linear-type S-bridged trinuclear complexes, [M'{M(aet or L-cys-N,S)$_3$}$_2$]$^{n+,n-}$, have been prepared by reacting with metal ions such as M' = Fe(III), Co(III), Co(II), and Ni(II).[2–4] In the linear-type trinuclear structure the central metal ion M' is situated in a distorted octahedral environment, coordinated by six sulfur atoms from the two terminal $fac(S)$-[M(aet or L-cys-N,S)$_3$]$^{0,3-}$ subunits, which has been confirmed by X-ray analyses for [Co{Co(aet)$_3$}$_2$]$^{3+}$,[2f] [Co{Co(L-cys-N,S)$_3$}$_2$]$^{3-}$,[3b] [Ni{Co(aet)$_3$}$_2$]$^{2+}$,[2i] and [Co{Ir(aet)$_3$}$_2$]$^{3+}$.[4d] These $fac(S)$ mononuclear complexes also react with metal ions such as Zn(II) and Cd(II) which prefer to take a tetrahedral coordination geometry, and the reaction products have long been assumed to be linear-type S-bridged trinuclear or tetranuclear complexes,[2b,d,e] although none of them have been structurally characterized.

This situation changed with our discovery of a new class of T-cage-type S-bridged heptanuclear complex with a "defective" [Zn$_3$HO]$^{5+}$ core, [{Rh(aet)$_3$}$_4$Zn$_3$OH]$^{5+}$, which is readily formed from $fac(S)$-[Rh(aet)$_3$] and Zn(II) in water.[5] Furthermore, we have recently found that the reaction of $fac(S)$-[Co(aet)$_3$] with Zn(II) in water does not give a linear-type but a T-cage-type S-bridged octanuclear complex with a "complete" [Zn$_4$O]$^{6+}$ core, [{Co(aet)$_3$}$_4$Zn$_4$O]$^{6+}$, by way of a T-cage-type heptanuclear complex with a "defective" core.[7] In the T-cage-type S-bridged structure either of Δ- or Λ-$fac(S)$-[M(aet)$_3$] (M = Co(III), Rh-(III)) is incorporated, forming only the $\Delta\Delta\Delta\Delta$ and $\Lambda\Lambda\Lambda\Lambda$ isomers which are spontaneously resolved. This is in wholly contrast to the fact that the linear-type trinuclear complexes [M'{M(aet)$_3$}$_2$]$^{n+}$ give all three possible isomers, $\Delta\Delta$, $\Lambda\Lambda$, and $\Delta\Lambda$, which may be separated and optically resolved by fractional recrystallization and/or column chromatography.

Scheme 1

fac(S) Mononuclear

Co(III)／H$_2$O   Zn(II)／H$_2$O

Linear-Type Trinuclear

Zn, Zn(II)／H$_2$O →

T-Cage-Type Octanuclear

The unique structure and properties of these T-cage-type S-bridged complexes prompted us to prepare novel T-cage-type octanuclear complexes composed of four *fac(S)*-[Rh(aet)$_3$] or *fac(S)*-[Rh(L-cys-N,S)$_3$]$^{3-}$ subunits and a "complete" [Zn$_4$O]$^{6+}$ core. In this paper we report on the synthesis, structure, and chemical characterization of the T-cage-type S-bridged octa-nuclear complexes, [{Rh(aet)$_3$}$_4$Zn$_4$O]$^{6+}$ and [{Rh(L-cys-N,S)$_3$}$_4$Zn$_4$O]$^{6-}$, along with the conversion of the linear-type S-bridged trinuclear structure in [Co{Rh(aet)$_3$}$_2$]$^{3+}$ to the T-cage-type octanuclear structure in [{Rh(aet)$_3$}$_4$Zn$_{3.7}$Co$_{0.3}$O]$^{6+}$ (Scheme 1).[6]

Experimental Section

Preparation of Complexes. *fac(S)*-[Rh(aet)$_3$]. This complex was prepared by a modified method described in the literature.[10] To a deoxygenated solution containing 5.2 g (0.13 mol) of NaOH and 10.0 g (0.13 mol) of 2-aminoethanethiol (Haet) in 140 cm^3 of water was added 2.0 g (0.01 mol) of RhCl$_3$. The mixture was stirred at 90 °C for 3 h under a nitrogen atmosphere, during which time a pale yellow precipitate appeared. This precipitate was collected by filtration and washed with a large amount of water, methanol, and then acetone. Yield: 1.9 g (61%).

Δ$_{LLL}$-*fac(S)*-H$_3$[Rh(L-cys-*N,S*)$_3$]. This complex was prepared by a modified method described in the literature.[4b] To a deoxygenated solution containing 5.2 g (0.13 mol) of NaOH and 15.8 g (0.13 mol) of L-cysteine (L-H$_2$cys) in 140 cm^3 of water was added 2.0 g (0.01 mol) of RhCl$_3$. The mixture was stirred at 90 °C for 6 h under a nitrogen atmosphere. After the reaction solution was cooled to room temperature, its pH was adjusted to ca. 2 with 1 mol dm^{-3} HCl. The resulting crude orange precipitate was collected by filtration, followed by suspension in 300 cm^3 of 1 mol dm^{-3} HCl. The remaining yellow complex was collected by filtration and washed with a large amount of 1 mol dm^{-3} HCl, methanol, and then acetone. Yield: 1.0 g (22%).

[{Rh(aet)$_3$}$_4$Zn$_4$O]$^{6+}$ (1). To a suspension containing 0.2 g (0.6 mmol) of *fac(S)*-[Rh(aet)$_3$] in 10 cm^3 of water was added 0.5 g (6.1 mmol) of ZnO and 0.3 g (1.3 mmol) of ZnBr$_2$. The mixture was stirred at room temperature for 2 h and then filtered to remove insoluble ZnO. To the yellow filtrate was added 2 g of NaBr in 8 cm^3 of water, followed by cooling in a refrigerator overnight. The resulting fine yellow crystals (1Br$_6$·NaBr·8H$_2$O) were collected by filtration. Yield: 0.28 g (80%). Anal. Calcd for [{Rh(C$_2$H$_6$NS)$_3$}$_4$Zn$_4$O]Br$_6$·NaBr·8H$_2$O: C, 12.38; H, 3.81; N, 7.22. Found: C, 12.33; H, 3.76; N, 6.97. This complex was also formed by stirring the aqueous mixture of *fac(S)*-[Rh(aet)$_3$] and ZnBr$_2$ at 60 °C for 6 h.

Recrystallization of 1Br$_6$·NaBr·8H$_2$O from water at room temperature gave spontaneously resolved yellow crystals (1Br$_6$·9H$_2$O). Each crystal that was picked up from the bulk showed a positive or a negative CD sign with the same |Δε| value at the same wavelength. One of these crystals, which showed a negative CD value at 350 nm, was used for X-ray analysis. Anal. Calcd for [{Rh(C$_2$H$_6$NS)$_3$}$_4$Zn$_4$O]Br$_6$·9H$_2$O: C, 12.84; H, 4.04; N, 7.49; Zn, 11.66; Rh, 18.34. Found: C, 12.77; H, 4.04; N, 7.36; Zn, 11.22; Rh, 17.55.

The chloride and nitrate salts of **1**, which were also spontaneously resolved, were prepared using ZnCl$_2$ or Zn(NO$_3$)$_2$ instead of ZnBr$_2$. Anal. Calcd for [{Rh(C$_2$H$_6$NS)$_3$}$_4$Zn$_4$O]Cl$_6$·3NaCl·9H$_2$O: C, 13.39; H, 4.21; N, 7.81. Found: C, 13.47; H, 4.16; N, 7.75. Calcd for [{Rh(C$_2$H$_6$NS)$_3$}$_4$Zn$_4$O](NO$_3$)$_6$·6H$_2$O: C, 13.84; H, 4.06; N, 11.43. Found: C, 13.55; H, 3.98; N, 11.61.

Δ$_{LLL}$Δ$_{LLL}$Δ$_{LLL}$Δ$_{LLL}$-[{Rh(L-cys-*N,S*)$_3$}$_4$Zn$_4$O]$^{6-}$ (2). To a suspension containing 0.2 g (0.4 mmol) of Δ$_{LLL}$-H$_3$[Rh(L-cys-*N,S*)$_3$] in 10 cm^3 of water was added 0.37 g (4.5 mmol) of ZnO and 0.21 g (0.9 mmol) of ZnBr$_2$. The pH of the mixture was adjusted to ca. 9 using 1 mol dm^{-3} KOH aqueous solution. The mixture was stirred at room temperature for 2 h and then filtered to remove insoluble ZnO. The yellow filtrate was concentrated to a small volume with a rotary evaporator, followed by storing in a refrigerator for 2 days. The resulting yellow crystals (K$_6$2·18H$_2$O), which showed a negative CD value at 350 nm, were collected by filtration. Yield: 0.13 g (45%). Anal. Calcd for K$_6$[{Rh(C$_3$H$_5$NO$_2$S)$_3$}$_4$Zn$_4$O]·18H$_2$O: C, 16.15; H, 3.61; N, 6.28. Found: C, 16.25; H, 3.63; N, 6.23.

[{Rh(aet)$_3$}$_4$Zn$_{3.7}$Co$_{0.3}$O]$^{6+}$ (3). To a dark brown solution containing 0.5 g (0.5 mmol) of [Co^{III}{Rh(aet)$_3$}$_2$](NO$_3$)$_3$[4b] in 50 cm^3 of water was added 1.5 g of Zn powder, and the mixture was stirred at room temperature. A red precipitate of [Co^{II}{Rh(aet)$_3$}$_2$](NO$_3$)$_2$[4b] appeared in a few minutes, which gradually dissolved to give a pale reddish brown solution after 1 h. When 1.5 g (6.7 mmol) of ZnBr$_2$ dissolved in a small amount of water was added to the reddish brown solution, the solution color immediately changed to green. After the mixture was stirred at room temperature for 1 h, unreacted Zn powder was filtered off and the green filtrate was allowed to stand in a refrigerator for 1 day. The resulting fine green crystals (3Br$_6$·8H$_2$O) were collected by filtration. Yield: 0.35 g (61%). Anal. Calcd for [{Rh(C$_2$H$_6$NS)$_3$}$_4$Zn$_{3.7}$Co$_{0.3}$O]Br$_6$·8H$_2$O: C, 12.96; H, 3.99; N, 7.56; Zn, 10.88; Co, 0.79; Rh 18.50. Found: C, 12.79; H, 4.20; N, 7.44; Zn, 10.42; Co, 0.76; Rh, 17.78.

Recrystallization of 3Br$_6$·8H$_2$O from water at room temperature gave spontaneously resolved green crystals. Each crystal that was picked up from the bulk showed a positive or a negative CD sign with the same |Δε| value at the same wavelength. One of these crystals, which showed a negative CD value at 350 nm, was used for X-ray analysis. The same reaction using ΔΔ-[Co{Rh(aet)$_3$}$_2$](NO$_3$)$_3$[4b] instead of [Co{Rh(aet)$_3$}$_2$](NO$_3$)$_3$ produced only the (−)$^{CD}_{350}$-ΔΔΔΔ isomer of **3**.

The chloride and nitrate salts of **3**, which were also spontaneously resolved, were prepared using ZnCl$_2$ or Zn(NO$_3$)$_2$ instead of ZnBr$_2$. Anal. Calcd for [{Rh(C$_2$H$_6$NS)$_3$}$_4$Zn$_{3.7}$Co$_{0.3}$O]Cl$_6$·3NaCl·9H$_2$O: C, 13.39; H, 4.21; N, 7.81. Found: C, 13.40; H, 4.16; N, 7.93. Calcd for [{Rh(C$_2$H$_6$NS)$_3$}$_4$Zn$_{3.7}$Co$_{0.3}$O](NO$_3$)$_6$·6H$_2$O: C, 13.84; H, 4.06; N, 11.43. Found: C, 13.62; H, 3.89; N, 11.84.

Measurements. The electronic absorption spectra were recorded with a Jasco UVIDEC-505 or UVIDEC-610C spectrophotometer, and the CD spectra with a Jasco J-600 spectropolarimeter. The elemental analyses (C, H, N) were performed by the Analysis Center of the University of Tsukuba. The concentrations of Rh, Zn, and Co in the complexes were determined by plasma emission spectral analyses with a Nippon Jarrel-Ash ICPA-575 ICP spectrophotometer. The ^{13}C NMR spectra were recorded with a Bruker AM-500 NMR spectrometer at the probe temperature in D$_2$O. Sodium 4,4-dimethyl-4-silapentane-1-sulfonate (DSS) was used as the internal reference.

X-ray Structure Determination. Single-crystal X-ray diffraction experiments were performed on an Enraf-Nonius CAD4 diffractometer with a graphite-monochromatized Mo Kα radiation (λ = 0.710 73 Å). Unit cell parameters were determined by a least-squares refinement, using the setting angles of 25 reflections in the ranges of 15 < 2θ < 17° (1Br$_6$) and 20 < 2θ < 24° (3Br$_6$). The intensity data were collected by the ω–2θ scan mode up to 2θ = 50° (+h,+k,+l). A total of 6679 (1Br$_6$) and 6499 (3Br$_6$) reflections were collected, 1816 (1Br$_6$) and 1670 (3Br$_6$) of which were considered to observed ($F_o > 5\sigma(F_o)$). Data reduction and application of Lorentz, polarization, and decomposition corrections were carried out by using the Enraf-Nonius Structure Determination Package.[11] Crystal absorptions were monitored for using a series of ψ-scans, but no corrections were applied because absorptions were not significant (transmission factors 0.944–1.000 for **1** and 0.968–0.998 for **3**).

The systematic absences led to the choice of either the space group $P2_12_12_1$ (No. 19) or $P2_13$ (No. 198) for each of 1Br$_6$ and 3Br$_6$. When each structure was solved by direct methods[11] and conventional difference Fourier techniques for the space group $P2_12_12_1$, all atoms of the complex

(10) Kita, M.; Yamanari, K.; Shimura, Y. *Bull. Chem. Soc. Jpn.* **1983**, *56*, 3272.

(11) *Enraf Nonius Structure Determination Package (SDP)*; Enraf Nonius: Delft, Holland, 1978.

Table 1. Crystallographic Data[a] for $(-)_{350}^{CD}$-[{Rh(aet)$_3$}$_4$Zn$_4$O]-Br$_6$·9H$_2$O ($(-)_{350}^{CD}$-1Br$_6$·9H$_2$O) and $(-)_{350}^{CD}$-[{Rh(aet)$_3$}$_4$Zn$_{3.7}$Co$_{0.3}$O]-Br$_6$·8H$_2$O ($(-)_{350}^{CD}$--3Br$_6$·8H$_2$O)

	$(-)_{350}^{CD}$-1Br$_6$·9H$_2$O	$(-)_{350}^{CD}$-3Br$_6$·8H$_2$O
chem formula	C$_{24}$H$_{90}$N$_{12}$O$_{10}$S$_{12}$Zn$_4$-Br$_6$Rh$_4$	C$_{24}$H$_{88}$N$_{12}$O$_9$S$_{12}$Zn$_4$-Br$_6$Rh$_4$
fw	2244.5	2226.5
cryst color	yellow	green
cryst size	0.10 × 0.20 × 0.25	0.10 × 0.18 × 0.25
space group	$P2_13$ (No. 198)	$P2_13$ (No. 198)
a, Å	19.017(1)	18.922(1)
v, Å^3	6876.9(4)	6775.3(4)
Z	4	4
ρ_{calc}, g cm^{-3}	2.17	2.18
μ, cm^{-1}	59.9	59.9
R^b	0.0519	0.0495
$R_w{}^{c,d}$	0.0475	0.0430
$R'{}^{b,f}$	0.0615	0.0602
$R'_w{}^{c,e,f}$	0.0587	0.0553
R'/R^g	1.18	1.22

[a] $T = 23$ °C; λ(Mo Kα) = 0.710 73 Å. [b] $R = \sum(||F_o| - |F_c||)/\sum(|F_o|)$. [c] $R_w = (\sum w(|F_o| - |F_c|)^2/\sum w(|F_o|)^2)^{1/2}$. [d] $w = 3.52/(\sigma^2(F_o + (4.5 \times 10^{-4})|F_o|^2)$ for 1 and $w = 2.47/(\sigma^2(F_o + (4.5 \times 10^{-4})|F_o|^2)$ for 3. [e] $w = 3.69/(\sigma^2(F_o + (5.3 \times 10^{-4})|F_o|^2)$ for 1 and $w = 2.68/(\sigma^2(F_o + (5.1 \times 10^{-4})|F_o|^2)$ for 3. [f] Refinement in the enantiomeric parameters. [g] The enantiomer selected is correct with greater than 99.5% certainty.[15]

cation existed almost on the positions expected for the site symmetry of $P2_13$. Hence, the space group was deduced to be $P2_13$, and this assignment was confirmed by the eventual structure refinement. Each structure for the space group $P2_13$ was solved by using the non-hydrogen atom positions of one-third of the formula unit obtained from the space group $P2_12_12_1$. Each atom of the mixed Zn/Co site (Zn:Co = 3.7:0.3) in 3Br$_6$ was refined as a Zn atom. In 1Br$_6$ two of four crystallographically independent Br atoms (Br1 and Br4) exhibited positional disorder. The RhB, ZnB, and O atoms in the complex cation and the Br atoms (Br2, Br3, Br4A, and Br4B for 1Br$_6$ and Br3 and Br4 for 3Br$_6$) were constrained to the special positions of symmetry 3. Each structure was refined by full-matrix least-squares techniques using SHELX76.[12] All non-hydrogen atoms were refined anisotropically, and hydrogen atoms were not included in the calculations. Scattering factors and anomalous dispersion corrections for Rh and Zn were taken from ref 13, while all others were supplied in SHELX76. Crystallographic data for 1Br$_6$ and 3Br$_6$ are summarized in Table 1, and non-hydrogen atom coordinates are listed in Tables 2 (1Br$_6$) and 3 (3Br$_6$). Listing of complete bond distances and angles and anisotropic thermal parameters have been deposited as supplementary materials.

Results and Discussion

Crystal Structures. X-ray structural analyses of the spontaneously resolved crystals, yellow $(-)_{350}^{CD}$-1Br$_6$ and green $(-)_{350}^{CD}$-3Br$_6$, revealed the presence of a discrete complex cation, bromide anions, and water molecules in each crystal. The total site occupancy factor of the bromide anions implies that the entire complex cations $(-)_{350}^{CD}$-1 and $(-)_{350}^{CD}$-3 are hexavalent (Tables 2 and 3). A perspective drawing of the entire complex cation for $(-)_{350}^{CD}$-1 is given in Figure 1a, and its polyhedral representation is depicted in Figure 1b. The selected bond lengths and angles for $(-)_{350}^{CD}$-1 and $(-)_{350}^{CD}$-3 are listed in Tables 4 and 5.

The entire complex cation $(-)_{350}^{CD}$-1 has crystallographically imposed C_3 symmetry, the RhB, O, and ZnB atoms lying on the 3-fold axis. As shown in Figure 1a, the complex cation consists of four approximately octahedral $fac(S)$-[Rh(aet)$_3$] subunits, four zinc atoms, and one central μ_4-oxygen atom. This is compatible with the plasma emission spectral analysis of 1Br$_6$ that gave the value of Rh:Zn = 4.0:4.0. The four zinc atoms are bound to the central oxygen atom in a tetrahedral geometry (ZnA–O–ZnA = 109.3(5)°, ZnA–O–ZnB = 109.6(5)°, ZnA–O = 1.963(6) Å,

(12) Sheldrick, G. M. *SHELX76, A Program for X-ray Crystal Structure Determination*; University of Cambridge: Cambridge, U.K., 1976.
(13) Cromer, D. T.; Waber, J. T. *International Tables for X-ray Crystallography*; Kynoch Press: Birmingham, U.K., 1974; Vol. IV.

Table 2. Final Atomic Coordinates and Equivalent Isotropic Thermal Parameters (Å^2) for $(-)_{350}^{CD}$-1Br$_6$·9H$_2$O

atom	x	y	z	B_{eq},[a] Å^2	occ
RhA	0.06441(6)	0.14370(6)	0.86489(6)	2.29(5)	
S1A	0.1671(2)	0.1437(2)	0.9320(2)	2.50(16)	
S2A	-0.0091(2)	0.1889(2)	0.9522(2)	2.40(16)	
S3A	0.0376(2)	0.0269(2)	0.8885(2)	2.85(17)	
N1A	-0.0232(7)	0.1398(8)	0.7983(8)	4.14(72)	
N2A	0.1286(7)	0.1114(7)	0.7811(7)	3.14(62)	
N3A	0.0819(8)	0.2507(7)	0.8412(6)	3.64(66)	
C1A	0.2235(9)	0.0946(11)	0.8707(9)	4.68(94)	
C2A	0.2034(12)	0.1140(13)	0.7955(10)	6.1(12)	
C3A	0.0070(10)	0.2827(8)	0.9395(9)	3.88(82)	
C4A	0.0791(9)	0.2952(9)	0.9064(9)	3.43(78)	
C5A	-0.0468(14)	0.0227(13)	0.8441(13)	7.3(14)	
C6A	-0.0479(18)	0.0677(16)	0.7813(13)	9.7(18)	
RhB	0.18952(6)	0.18952(6)	0.18952(6)	1.89(4)	$^1/_3$
S1B	0.2375(2)	0.1011(2)	1.1184(2)	2.53(17)	
N1B	0.2527(7)	0.1499(7)	1.2722(7)	3.11(63)	
C1B	0.3065(9)	0.1517(11)	1.0777(11)	4.9(10)	
C2B	0.2231(11)	0.0887(14)	1.3068(12)	6.7(13)	
ZnA	0.16218(9)	0.06694(9)	1.02862(9)	2.11(7)	
ZnB	0.00673(9)	0.00673(9)	0.00673(9)	2.30(6)	$^1/_3$
O	0.0659(5)	0.0659(5)	0.0659(5)	2.22(29)	$^1/_3$
Br1A	0.4262(2)	0.1937(2)	0.2495(2)	6.45(18)	0.8
Br1B	0.4805(15)	0.1722(12)	0.2647(8)	12.4(14)	0.2
Br2	0.4144(3)	0.4144(3)	0.4144(3)	17.33(36)	$^1/_3$
Br3	-0.0780(1)	0.4220(1)	0.0780(1)	4.02(6)	$^1/_3$
Br4A	-0.2943(2)	0.2057(2)	0.2943(2)	5.27(14)	$^2/_9$
Br4B	-0.2703(7)	0.2297(7)	0.2703(7)	8.37(63)	$^1/_9$
O1W	0.8216(11)	0.1587(10)	0.4436(10)	10.3(12)	
O2W	-0.3864(9)	0.5302(10)	0.2772(9)	8.4(10)	
O3W	0.4137(10)	0.5548(12)	0.5272(12)	11.4(14)	

[a] B_{eq} is the arithmetic mean of the principal axes of the thermal ellipsoid.

Table 3. Final Atomic Coordinates and Equivalent Isotropic Thermal Parameters (Å^2) for $(-)_{350}^{CD}$-3Br$_6$·8H$_2$O

atom	x	y	z	B_{eq},[a] Å^2	occ
RhA	0.05947(6)	0.14353(6)	0.86134(6)	2.05(5)	
S1A	0.1645(2)	0.1438(2)	0.9277(2)	2.27(17)	
S2A	-0.0142(2)	0.1872(2)	0.9505(2)	2.41(17)	
S3A	0.0354(2)	0.0240(2)	0.8846(2)	2.60(18)	
N1A	-0.0303(7)	0.1391(8)	0.7930(7)	3.56(70)	
N2A	0.1246(7)	0.1124(8)	0.7763(7)	3.10(67)	
N3A	0.0768(7)	0.2543(7)	0.8392(7)	3.05(65)	
C1A	0.2192(9)	0.0964(11)	0.8646(10)	4.21(93)	
C2A	0.2012(9)	0.1186(11)	0.7907(9)	3.99(96)	
C3A	0.0008(10)	0.2833(8)	0.9391(10)	3.66(86)	
C4A	0.0721(10)	0.2960(8)	0.9043(9)	3.05(81)	
C5A	-0.0493(12)	0.0173(12)	0.8353(10)	5.6(12)	
C6A	-0.0531(20)	0.0641(14)	0.7776(20)	13.2(25)	
RhB	0.18739(6)	0.18739(6)	0.18739(6)	1.85(4)	$^1/_3$
S1B	0.2347(2)	0.0969(2)	1.1175(2)	2.20(17)	
N1B	0.2476(7)	0.1504(7)	1.2723(6)	2.39(59)	
C1B	0.3108(8)	0.1437(10)	1.0780(9)	3.33(80)	
C2B	0.2232(10)	0.0779(10)	1.2981(9)	3.40(86)	
ZnA	0.15971(9)	0.0656(1)	1.02461(9)	2.10(8)	
ZnB	0.0033(1)	0.0033(1)	0.0033(1)	2.20(6)	$^1/_3$
O	0.0626	0.0626(5)	0.0626(5)	1.63(28)	$^1/_3$
Br1	0.4222(1)	0.1917(2)	0.2488(1)	6.62(14)	
Br2	0.3830(5)	0.4393(9)	0.4301(5)	11.9(10)	$^1/_3$
Br3	-0.0823(1)	0.4177(1)	0.0823(1)	3.75(7)	$^1/_3$
Br4	-0.3023(2)	0.1977(2)	0.3023(2)	8.00(14)	$^1/_3$
O1W	0.8110(13)	0.1598(10)	0.4427(11)	12.1(15)	
O2W	-0.3952(10)	0.5215(10)	0.2899(11)	9.8(13)	
O3W	0.4176(13)	0.5469(18)	0.5264(19)	10.7(20)	$^2/_3$

[a] B_{eq} is the arithmetic mean of the principal axes of the thermal ellipsoid.

ZnB–O = 1.949(17) Å), and to this tetrahedral [Zn$_4$O]$^{6+}$ core the four $fac(S)$-[Rh(aet)$_3$] subunits are bound in a tetrahedral arrangement, completing the T-cage-type S-bridged octanuclear structure.[14] Each zinc atom takes an approximately tetrahedral geometry, coordinated by three sulfur atoms from three different

(14) The T symmetrical structure is understood by four C_3 axes passing through the Rh, O, and Zn atoms (one of them is crystallographically imposed).
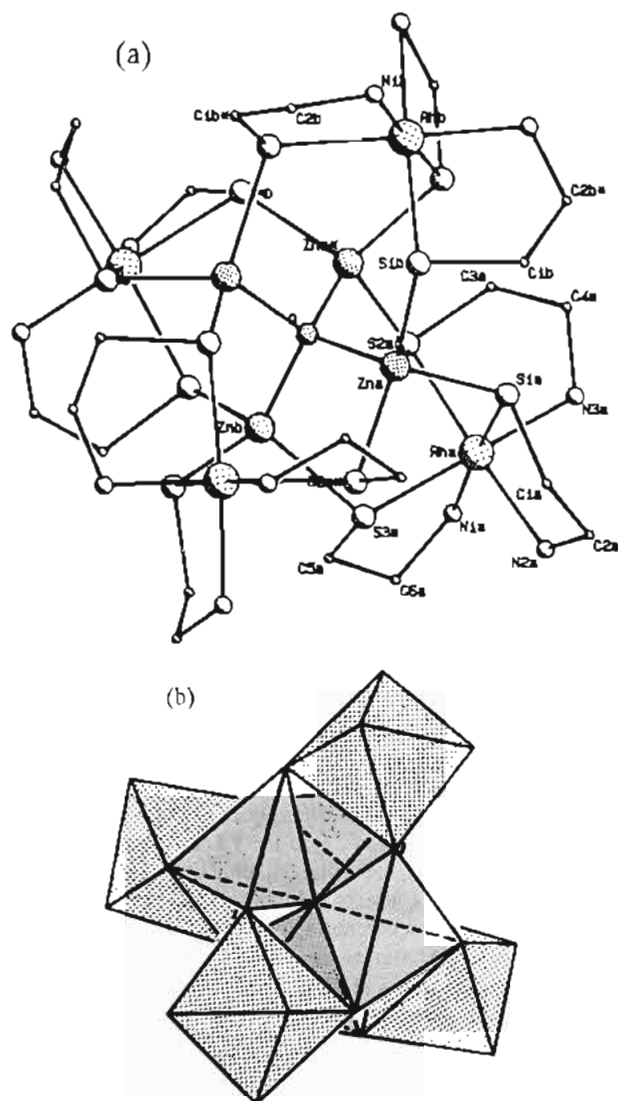
(a)

(b)

Figure 1. Perspective view of $(-)^{CD}_{350}$-**1** with the atomic labeling scheme (a) and its polyhedral representation (b).

Table 4. Selected Bond Distances (Å) and Angles (deg) for $(-)^{CD}_{350}$-**1**Br$_6$·9H$_2$O

RhA–S1A	2.334(4)	S2A–ZnA	2.353(4)
RhA–S2A	2.333(4)	S3A–ZnB	2.355(4)
RhA–S3A	2.324(4)	RhB–S1B	2.343(4)
RhA–N1A	2.094(14)	RhB–N1B	2.118(13)
RhA–N2A	2.099(12)	S1B–ZnA	2.320(4)
RhA–N3A	2.111(13)	ZnA–O	1.963(6)
S1A–ZnA	2.348(4)	ZnB–O	1.949(17)
S1A–RhA–S2A	96.4(1)	S1B–RhB–S1B	95.1(1)
S1A–RhA–S3A	94.5(1)	S1B–RhB–N1B	87.3(4)
S2A–RhA–S3A	94.8(1)	N1B–RhB–N1B	92.5(5)
S1A–RhA–N1A	175.5(4)	RhB–S1B–ZnA	112.7(2)
S2A–RhA–N1A	88.1(4)	S1A–ZnA–S2A	109.3(1)
S3A–RhA–N1A	84.7(4)	S1A–ZnA–S1B	112.1(1)
S1A–RhA–N2A	85.9(4)	S2A–ZnA–S1B	110.5(1)
S2A–RhA–N2A	174.8(4)	S3A–ZnB–S3A	110.6(1)
S3A–RhA–N2A	89.7(4)	S1A–ZnA–O	109.0(1)
S1A–RhA–N3A	89.1(4)	S2A–ZnA–O	107.6(3)
S2A–RhA–N3A	83.8(4)	S1B–ZnA–O	108.2(4)
S3A–RhA–N3A	176.2(4)	S3A–ZnB–O	108.3(1)
N1A–RhA–N2A	89.6(6)	ZnA–O–ZnA	109.3(5)
N1A–RhA–N3A	91.7(6)	ZnA–O–ZnB	109.6(5)
N2A–RhA–N3A	91.6(5)		

fac(*S*)-[Rh(aet)$_3$] subunits and an oxygen atom at the center of the octanuclear structure. As seen in Figure 1a, the bonding direction of the three sulfur atoms of one *fac*(*S*)-[Rh(aet)$_3$] subunit toward the trigonal Zn$_3$ face of the [Zn$_4$O]$^{6+}$ core is approximately

Table 5. Selected Bond Distances (Å) and Angles (deg) for $(-)^{CD}_{350}$-**3**Br$_6$·8H$_2$O

RhA–S1A	2.351(4)	S2A–ZnA	2.357(6)
RhA–S2A	2.339(4)	S3A–ZnB	2.360(4)
RhA–S3A	2.349(4)	RhB–S1B	2.341(4)
RhA–N1A	2.137(14)	RhB–N1B	2.090(12)
RhA–N2A	2.111(13)	S1B–ZnA	2.336(4)
RhA–N3A	2.162(14)	ZnA–O	1.974(6)
S1A–ZnA	2.357(4)	ZnB–O	1.942(16)
S1A–RhA–S2A	96.7(1)	N2A–RhA–N3A	92.0(5)
S1A–RhA–S3A	93.8(1)	S1B–RhB–S1B	94.8(1)
S2A–RhA–S3A	95.2(1)	S1B–RhB–N1B	88.9(4)
S1A–RhA–N1A	174.6(4)	N1B–RhB–N1B	91.2(5)
S2A–RhA–N1A	88.7(4)	S1A–ZnA–S2A	109.2(1)
S3A–RhA–N1A	85.5(4)	S1A–ZnA–S1B	113.8(2)
S1A–RhA–N2A	85.1(4)	S2A–ZnA–S1B	109.5(1)
S2A–RhA–N2A	175.1(4)	S1A–ZnA–O	109.7(1)
S3A–RhA–N2A	89.2(4)	S2A–ZnA–O	107.0(5)
S1A–RhA–N3A	88.5(4)	S1B–ZnA–O	107.4(4)
S2A–RhA–N3A	83.5(4)	S3A–ZnB–S3A	111.1(1)
S3A–RhA–N3A	177.5(4)	S3A–ZnB–O	107.8(1)
N1A–RhA–N2A	89.6(5)	ZnA–O–ZnA	108.8(4)
N1A–RhA–N3A	92.4(5)	ZnA–O–ZnB	110.1(4)

perpendicular to the trigonal S$_3$ face. This directionality indicates that *fac*(*S*)-[Rh(aet)$_3$] cannot function as a S-donating tridentate ligand to one tetrahedral zinc atom.

The complex cation **1**, [{Rh(aet)$_3$}$_4$Zn$_4$O]$^{6+}$, has two kinds of chiral centers, Δ or Λ for the *fac*(*S*)-[Rh(aet)$_3$] subunits and *R* or *S* for the sulfur atoms which become chiral on binding to zinc atoms. The absolute configurations for the spontaneously resolved $(-)^{CD}_{350}$ isomer of **1** was determined by the anomalous scattering technique. The structure containing Δ-*fac*(*S*)-[Rh(aet)$_3$] subunits in the complex cation is probably the correct choice, and its enantiomeric structure could be rejected at the 0.005 significance level by the Hamilton test (Table 1).[15] Thus, all 4 *fac*(*S*)-[Rh-(aet)$_3$] subunits take Δ and all 12 bridging sulfur atoms take *R* in $(-)^{CD}_{350}$-**1**, as shown in Figure 1.

The overall structure of **1** is essentially the same as that of the analogous Co^{III}$_4$Zn^{II}$_4$ T-cage-type octanuclear complex, [{Co(aet)$_3$}$_4$Zn$_4$O]$^{6+}$.[7] In particular, the bond distances and angles around zinc atoms (average Zn–S = 2.344(4) Å, Zn–O = 1.960-(17) Å, S–Zn–S = 110.6(1)°, and S–Zn–O = 108.3(4)°) in **1** (Table 4) are quite similar to those found in [{Co(aet)$_3$}$_4$Zn$_4$O]$^{6+}$ (average Zn–S = 2.342(3) Å, Zn–O = 1.948(12) Å, S–Zn–S = 111.7(1)°, and S–Zn–O = 107.2(3)°). The Rh–S (average 2.334-(4) Å) and Rh–N (average 2.106(14) Å) distances in **1** are ca. 0.1 Å longer than the Co–S (average 2.266(4) Å) and Co–N (average 2.004 Å) ones in [{Co(aet)$_3$}$_4$Zn$_4$O]$^{6+}$, respectively, as expected from the difference in covalent radii between rhodium and cobalt atoms. The S–Rh–N bite angles (average 85.4(4)°) are slightly smaller than the S–Co–N ones (average 86.4(3)°) in [{Co(aet)$_3$}$_4$Zn$_4$O]$^{6+}$, which results in the somewhat expanded S$_3$ and N$_3$ faces (average S–Rh–S = 95.2(1)° and N–Rh–N = 91.4(6)°), compared with those in [{Co(aet)$_3$}$_4$Zn$_4$O]$^{6+}$ (average S–Co–S = 93.8(1)° and N–Co–N = 90.2(4)°).

X-ray structural analysis indicated that green $(-)^{CD}_{350}$-**3**Br$_6$ is isostructural with yellow $(-)^{CD}_{350}$-**1**Br$_6$ (Tables 1–3), having a T-cage-type S-bridged octanuclear structure. The bond distances and angles in $(-)^{CD}_{350}$-**3** (Table 5) are in good agreement with those observed in $(-)^{CD}_{350}$-**1** (Table 4). However, the plasma emission spectral analysis of **3**Br$_6$ pointed out the presence of cobalt atoms in a ratio of Rh:Zn:Co = 4.0:3.7:0.3. In the electronic absorption spectrum **3** exhibits a characteristic absorption band composed of three components at ca. 14.5 × 10^3 cm^{-1}, although its absorption spectrum in the energy region higher than 20 × 10^3 cm^{-1} coincides with that of **1** (Figure 2 and Table 6). A quite similar absorption band has been observed for the tetrahedral Co(II) complexes
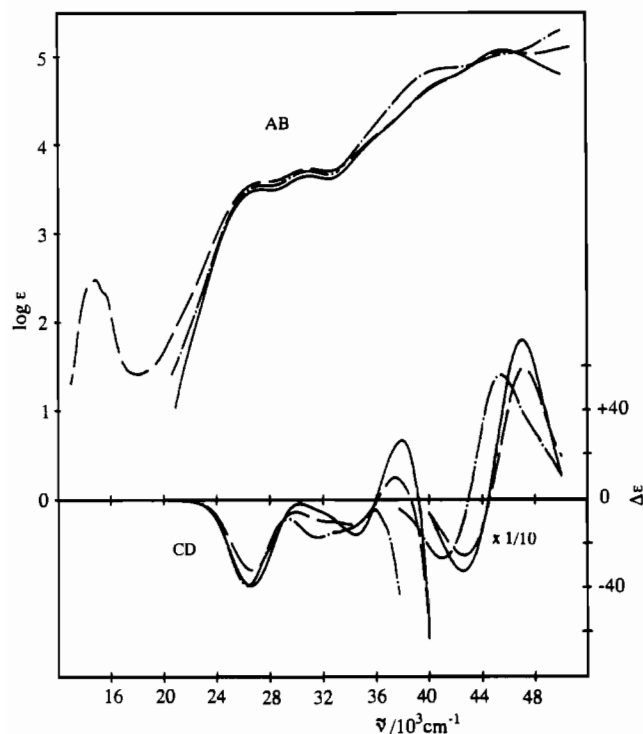
(15) Hamilton, W. C. *Acta Crystallogr.* **1965**, *18*, 502.

Figure 2. Electronic absorption and CD spectra of $\Delta\Delta\Delta\Delta$-[{Rh-(aet)$_3$}$_4$Zn$_4$O]$^{6+}$ ((-)$^{CD}_{350}$-1) (—), $\Delta_{LLL}\Delta_{LLL}\Delta_{LLL}\Delta_{LLL}$-[{Rh(L-cys-$N$,$S$)$_3$}$_4Zn_4$O]$^{6-}$ (2) (- · -), and $\Delta\Delta\Delta\Delta$-[{Rh(aet)$_3$}$_4$Zn$_{3.7}$Co$_{0.3}$O]$^{6+}$ ((-)$^{CD}_{350}$-3) (- -). ϵ values are given in units of mol^{-1} dm^3 cm^{-1}.

having a Co^{II}S$_4$ chromophore,[16] which has been assigned as a spin-allowed d–d transition ($^4A_2$(F) → $^4T_1$(P)). Accordingly, 3 is determined to be the T-cage-type octanuclear complex with a [Zn$_{3.7}$Co$_{0.3}$O]$^{6+}$ core, [{Rh(aet)$_3$}$_4$Zn$_{3.7}$Co$_{0.3}$O]$^{6+}$, where a slight amount of Co(II) is trapped in a tetrahedral coordination geometry in place of Zn(II). For the spontaneously resolved (-)$^{CD}_{350}$ isomer of 3, the chiral configurations are assigned to Δ for the 4 $fac(S)$-[Rh(aet)$_3$] subunits and R for the 12 bridging sulfur atoms (Table 1), as in the case of (-)$^{CD}_{350}$-1. This assignment is supported by the fact that (-)$^{CD}_{350}$-1 and (-)$^{CD}_{350}$-3 exhibit CD spectra quite similar to each other (Figure 2).

Synthesis and Characterization. The reaction of $fac(S)$-[Rh-(aet)$_3$] with a mixture of Zn^{2+} and ZnO in water at room temperature gave a T-cage-type S-bridged octanuclear complex with a "complete" [Zn$_4$O]$^{6+}$ core, [{Rh(aet)$_3$}$_4$Zn$_4$O]$^{6+}$ (1). 1 can also be prepared from $fac(S)$-[Rh(aet)$_3$] and Zn^{2+} in water at a high temperature (ca. 60 °C). Since the reaction solution of $fac(S)$-[Rh(aet)$_3$] and Zn^{2+} turned from neutral to acidic (ca. pH = 3), it is probable to consider that the central oxide in 1 comes from water. The stability of the T-cage-type S-bridged structure with a "complete" [Zn$_4$O]$^{6+}$ core besides the affinity of Zn(II) toward oxygen atom may be a significant factor of pulling hydrogen ions off water, which would be promoted by adding the potentially strong base of ZnO.

A similar reaction of Δ_{LLL}-$fac(S)$-[Rh(L-cys-N,S)$_3$]$^{3-}$ with Zn^{2+} and ZnO in water produced 2, which shows a negative CD value at 350 nm. As illustrated in Figure 2, the absorption and CD spectra of 2 are quite similar to those of the (-)$^{CD}_{350}$-$\Delta\Delta\Delta\Delta$ isomer of 1 over the whole region. Furthermore, in the ^{13}C NMR spectrum 2 gives three signals (δ 37.48, 67.67, 177.37) due to methylene, methine, and carboxylate carbon atoms of the L-cys ligands. From these facts and elemental analysis, 2 can be confidently assigned as $\Delta_{LLL}\Delta_{LLL}\Delta_{LLL}\Delta_{LLL}$-[{Rh(L-cys-$N$,$S$)$_3$}$_4$-

(16) (a) Lane, R. W.; Ibers, J. A.; Frankel, R. B.; Papaefthymiou, G. C.; Holm, R. H. *J. Am. Chem. Soc.* **1977**, *99*, 84. (b) Nakata, M.; Ueyama, N.; Nakamura, A.; Nozawa, T.; Hatano, M. *Inorg. Chem.* **1983**, *22*, 3028. (c) Dorfman, J. R.; Rao, Ch. P.; Holm, R. H. *Inorg. Chem.* **1985**, *24*, 453.

Zn$_4$O]$^{6-}$ with a T symmetrical structure; that is, $fac(S)$-[Rh(L-cys-N,S)$_3$]$^{3-}$ having free carboxylate groups can be incorporated in the T-cage-type octanuclear structure with retention of the Δ_{LLL} configuration.

The reaction of the linear-type S-bridged trinuclear complex, [Co^{III}{Rh(aet)$_3$}$_2$]$^{3+}$, with Zn powder in water at room temperature, followed by the addition of Zn^{2+}, produced a T-cage-type complex with [Zn$_{3.7}$Co$_{0.3}$O]$^{6+}$ core, [{Rh(aet)$_3$}$_2$Zn$_{3.7}$Co$_{0.3}$O]$^{6+}$ (3), by way of [Co^{II}{Rh(aet)$_3$}$_2$]$^{2+}$. Considering that only the (-)$^{CD}_{350}$-$\Delta\Delta\Delta\Delta$ isomer of 3 was derived from $\Delta\Delta$-[Co{Rh-(aet)$_3$}$_2$]$^{3+}$, it is seen that the conversion of a linear- to a cage-type S-bridged structure occurs with retention of the absolute configuration of the $fac(S)$-[Rh(aet)$_3$] subunits.

All the chloride, bromide, and nitrate salts of 1 and 3 were subject to spontaneous resolution, and each complex gave two optical isomers, (+)$^{CD}_{350}$ and (-)$^{CD}_{350}$, which show CD spectra enantiomeric to each other. Since the (-)$^{CD}_{350}$ isomer for each of 1 and 3 was determined by X-ray crystallography to take the Δ configuration for all the four $fac(S)$-[Rh(aet)$_3$] subunits, the (+)$^{CD}_{350}$ isomer for each of 1 and 3 is assigned to take the $\Lambda\Lambda\Lambda\Lambda$ configuration. Molecular model examinations reveal that there exist significant nonbonding interactions of the aet chelate rings among the $fac(S)$-[Rh(aet)$_3$] subunits when the absolute configurations of the four $fac(S)$-[Rh(aet)$_3$] subunits are not uniform. Accordingly, either of the Δ or Λ isomer of $fac(S)$-[Rh(aet)$_3$] is selectively incorporated in each of 1 and 3, forming only the $\Delta\Delta\Delta\Delta$ and $\Lambda\Lambda\Lambda\Lambda$ isomers with a T symmetry. Consistent with this result, the ^{13}C NMR spectrum for each of 1 and 3 shows only two signals due to two kinds of methylene carbon atoms of the 12 aet ligands (δ 33.86 and 51.20 for 1 and δ 33.64 and 51.20 for 3 from DSS). The same stereochemical behavior has been recognized for the analogous [{Co(aet)$_3$}$_4$Zn$_4$O]$^{6+}$, and the spontaneous resolution commonly observed for the T-cage-type complexes may be related to the high symmetrical structure.

Electronic Absorption and CD spectra. The absorption spectra of the present T-cage-type complexes exhibit two spin-allowed d–d transition bands at ca. 27 × 10^3 and 31 × 10^3 cm^{-1} and two intense sulfur-to-rhodium charge-transfer (CT) bands at ca. 41 × 10^3 and 46 × 10^3 cm^{-1} in the near-UV region (Figure 2 and Table 6). A similar absorption spectral feature has been observed for the analogous [{Co(aet)$_3$}$_4$Zn$_4$O]$^{6+}$,[7] although the d–d absorption bands (17.7 × 10^3 and 23.9 × 10^3 cm^{-1}) and the CT bands (30.6 × 10^3 and 38.0 × 10^3 cm^{-1}) were located at much lower energy than those for the present T-cage-type complexes. Figures 3 and 4 compare the absorption spectra of 1 and 2 with 4 mol of $fac(S)$-[Rh(aet)$_3$] and 4 mol of $fac(S)$-[Rh(L-cys-N,S)$_3$]$^{3-}$, respectively. The absorption curves of 1 and 2 roughly coincide with those of 4 mol of $fac(S)$-[Rh(aet)$_3$] and 4 mol of $fac(S)$-[Rh(L-cys-N,S)$_3$]$^{3-}$ over the whole region, indicating that the absorption spectra of 1 and 2 are dominated by the four $fac(S)$-[Rh(aet or L-cys-N,S)$_3$]$^{0,3-}$ subunits. However, some notable differences are observed in more minute detail. That is, the d–d absorption bands for 1 and 2 are clearer and shift to the higher energy side than those for the mononuclear $fac(S)$-[Rh-(aet or L-cys-N,S)$_3$]$^{0,3-}$, and furthermore, one broad sulfur-to-rhodium CT band for $fac(S)$-[Rh(aet or L-cys-N,S)$_3$]$^{0,3-}$ appears as two bands for 1 and 2.

Two kinds of CD contributions, one from 4 Δ-$fac(S)$-[Rh-(aet)$_3$] subunits and the other from 12 R configurational sulfur atoms, are expected for (-)$^{CD}_{350}$-$\Delta\Delta\Delta\Delta$-[{Rh(aet)$_3$}$_4$Zn$_4$O]$^{6+}$ ((-)$^{CD}_{350}$-1.) Beside these CD contributions, $\Delta_{LLL}\Delta_{LLL}\Delta_{LLL}\Delta_{LLL}$-[{Rh(L-cys-$N$,$S$)$_3$}$_4Zn_4$O]$^{6-}$ (2) has an additional vicinal CD contribution due to 12 R configurational carbon atoms of the L-cys ligands. As shown in Figure 2, the CD spectrum of 2 is quite similar to that of (-)$^{CD}_{350}$-1 over the whole region, implying that the vicinal CD contribution due to asymmetric carbon atoms is relatively small. Figure 4 compares the CD spectrum of 2 with that of 4 mol of Δ_{LLL}-$fac(S)$-[Rh(L-cys-N,S)$_3$]$^{3-}$. In the d–d

Table 6. Electronic Absorption and CD Spectral Data[a]

complex	abs max $\nu/10^3$ cm^{-1} (log ϵ/mol^{-1} dm^3 cm^{-1})	CD extrema $\nu/10^3$ cm^{-1} ($\Delta\epsilon$/mol^{-1} dm^3 cm^{-1})
(−)$_{350}^{CD}$-ΔΔΔΔ-[Rh{(aet)$_3$}$_4$Zn$_4$O]$^{6+}$ ((−)$_{350}^{CD}$-**1**)	27.47 (3.50)	26.60 (−31.01)
	31.06 (3.65)	34.48 (−11.90)
	41.7 (4.8, sh)	37.74 (+19.81)
	45.87 (5.06)	42.74 (−247.4)
		47.17 (+505.1)
Δ$_{LLL}$Δ$_{LLL}$Δ$_{LLL}$Δ$_{LLL}$-[Rh{L-cys-N,S}$_3$}$_4$Zn$_4$O]$^{6+}$ (**2**)	27.93 (3.54)	26.29 (−38.71)
	30.98 (3.71)	31.59 (−17.06)
	41.6 (4.9, sh)	32.9 (−14.9, sh)
	46.1 (5.0, sh)	40.92 (−264.5)
		45.37 (+588.0)
(−)$_{350}^{CD}$-ΔΔΔΔ-[Rh{(aet)$_3$}$_4$Zn$_{3.7}$Co$_{0.3}$O]$^{6+}$ ((−)$_{350}^{CD}$-**3**)	14.5 (2.45, sh)	26.74 (−29.26)
	14.86 (2.48)	34.48 (−10.97)
	15.5 (2.33, sh)	37.88 (+16.35)
	27.78 (3.61)	42.74 (−234.3)
	31.01 (3.74)	47.17 (+517.7)
	41.7 (4.7, sh)	
	45.66 (5.04)	
$fac(S)$-[Rh(aet)$_3$]	26.3 (2.9, sh)	
	30.03 (3.10)	
	44.05 (4.59)	
Δ$_{LLL}$-$fac(S)$-[Rh(L-cys-N,S)$_3$]$^{3-}$	26.3 (2.9, sh)	24.58 (−5.49)
	29.59 (3.05)	29.87 (−2.79)
	43.48 (4.61)	38.5 (+13.8, sh)
		43.03 (+71.92)
		47.57 (+44.23)

[a] The sh label denotes a shoulder.
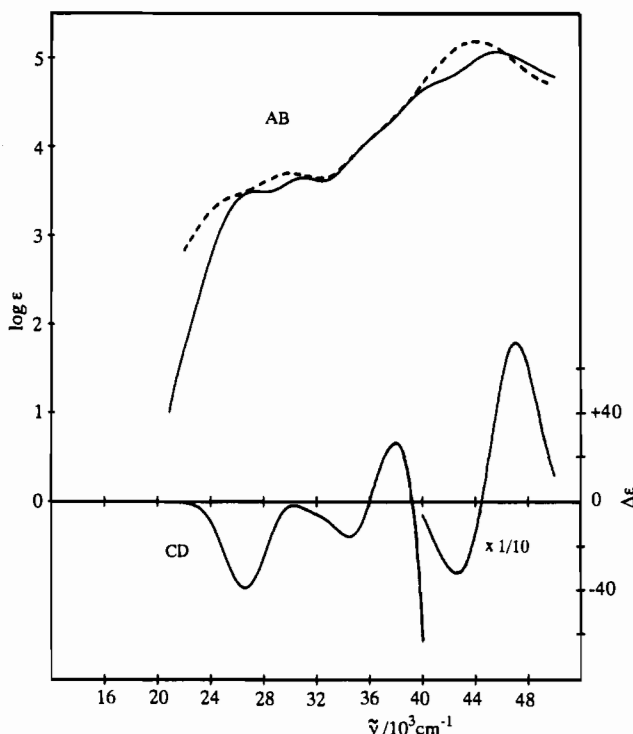
Figure 3. Electronic absorption and CD spectra of ΔΔΔΔ-[{Rh-(aet)$_3$}$_4$Zn$_4$O]$^{6+}$ ((−)$_{350}^{CD}$-**1**) (—) and $fac(S)$-[Rh(aet)$_3$] × 4 (- - -). ϵ values are given in units of mol^{-1} dm^3 cm^{-1}.

Figure 4. Electronic absorption and CD spectra of Δ$_{LLL}$Δ$_{LLL}$Δ$_{LLL}$Δ$_{LLL}$-[{Rh(L-cys-N,S)$_3$}$_4$Zn$_4$O]$^{6-}$ (**2**) (—) and Δ$_{LLL}$-$fac(S)$-[Rh(L-cys-N,S)$_3$]$^{3-}$ × 4 (− −). ϵ values are given in units of mol^{-1} dm^3 cm^{-1}.

absorption band region (22 × 10^3–33 × 10^3 cm^{-1}), the CD spectral behavior of **2** resembles that of 4 mol of Δ$_{LLL}$-$fac(S)$-[Rh(L-cys-N,S)$_3$]$^{3-}$, giving two positive CD bands. This suggests that in this region the CD contribution due to asymmetric sulfur atoms is minor and the CD pattern is dominated by the absolute configuration of the $fac(S)$-[Rh(L-cys-N,S)$_3$]$^{3-}$ subunits. In the sulfur-to-rhodium CT band region (40 × 10^3–48 × 10^3 cm^{-1}), however, the CD spectrum of **2** differs significantly from that of 4 mol of Δ$_{LLL}$-$fac(S)$-[Rh(L-cys-N,S)$_3$]$^{3-}$. That is, **2** gives a negative CD band at ca. 41 × 10^3 cm^{-1} and a positive one at ca. 45 × 10^3 cm^{-1}, while a major positive CD band is observed at ca.
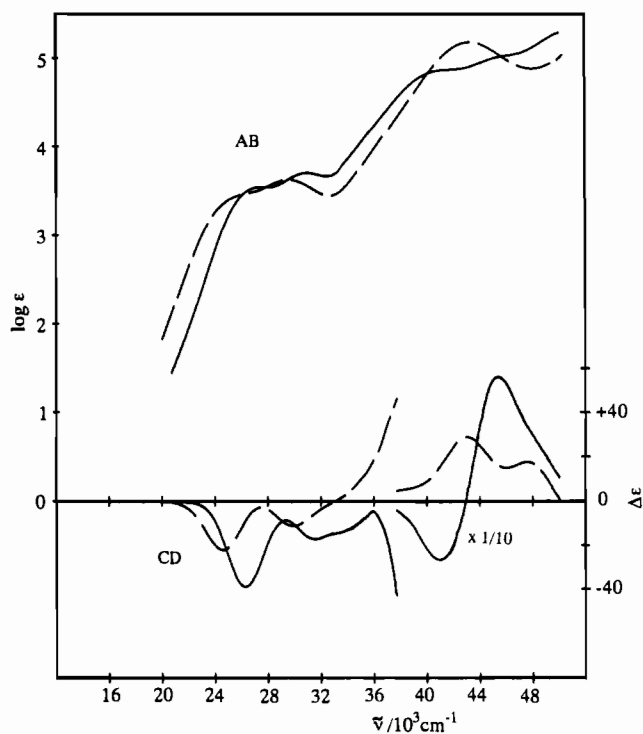
43 × 10^3 cm^{-1} for 4 mol of Δ$_{LLL}$-$fac(S)$-[Rh(L-cys-N,S)$_3$]$^{3-}$. Accordingly, it is considered that the asymmetric sulfur atoms in the T-cage-type octanuclear structure contribute dominantly to the CD spectra in the sulfur-to-rhodium CT band region.

1 and **2** with a [Zn$_4$O]$^{6+}$ core are fairly stable in water as is the analogous [{Co(aet)$_3$}$_4$Zn$_4$O]$^{6+}$;[7] no significant absorption and CD spectral changes with time were noticed for several days. This is also the case for **3** with a [Zn$_{3.7}$Co$_{0.3}$O]$^{6+}$ core, indicating that the Co(II) ion trapped in the cage-type structure is stabilized against oxidation. Since the octahedral Co(II) ion in the linear-type trinuclear complex, [Co^{II}{Rh(aet)$_3$}$_2$]$^{2+}$, readily suffers air

oxidation to give $[Co^{III}\{Rh(aet)_3\}_2]^{3+}$,[4b] it is reasonable to assume that the stabilization of Co(II) oxidation state in **3** is due to the tetrahedral coordination geometry constrained in the rigid T-cage-type octanuclear structure.

Concluding Remarks

In this work, the T-cage-type S-bridged octanuclear complexes with a "complete" $[Zn_4O]^{6+}$ core, $[\{Rh(aet\ or\ L\text{-}cys\text{-}N,S)_3\}_4Zn_4O]^{6+,6-}$ (**1** and **2**) were formed from $fac(S)$-$[Rh(aet\ or\ L\text{-}cys\text{-}N,S)_3]^{0,3-}$, Zn^{2+}, and ZnO in water under moderate conditions. Furthermore, the linear-type trinuclear structure in $[Co\{Rh(aet)_3\}_2]^{3+}$ was converted into the T-cage-type structure in $[\{Rh(aet)_3\}_4Zn_{3.7}Co_{0.3}O]^{6+}$ (**3**) by substitution of the bridging octahedral Co(III) with the tetrahedral Zn(II). These results suggest that the S-bridged polynuclear structure composed of $fac(S)$-$[Rh(aet\ or\ L\text{-}cys\text{-}N,S)_3]^{0,3-}$ subunits is highly dependent on the coordination geometry of metal ions incorporated in the polynuclear complexes and that the T-cage-type structure is possibly formed from $fac(S)$-$[M(aet\ or\ L\text{-}cys\text{-}N,S)_3]^{0,3-}$ and metal ions which take a tetrahedral coordination geometry. The T-cage-type structure discriminates the chiral configuration (Δ or Λ) of $fac(S)$-$[Rh(aet)_3]$ as well as that of $fac(S)$-$[Co(aet)_3]$, giving only the $\Delta\Delta\Delta\Delta$ and $\Lambda\Lambda\Lambda\Lambda$ isomers which are spontaneously resolved. Thus, using Zn(II) as a bridging metal ion, the optically active compounds containing total 16 chiral centers are available from the $fac(S)$-$[M(aet)_3]$ (M = Co(III), Rh(III)) molecules, which are unable to be optically resolved because of the poor solubility in any solvent.